RIDNet: Recursive Information Distillation Network for Color Image Denoising

Shengkai Zhuo[1†], Zhi Jin[1,2†], Wenbin Zou[1*], Xia Li[1]
[1]Shenzhen University, China
[2]Sun Yat-sen University, China
zhuoshengkai2017@email.szu.edu.cn, jinzhi_126@163.com, {wzou, lixia}@szu.edu.cn

Abstract

Color image denoising is more challenging in effectiveness when comparing with the grayscale one. Most existing methods play a certain role in efficiency or flexibility, but lack robustness to handle various noise levels, especially the severe noise. This keeps them away from being practically applied to color image denoising. To address this issue, we propose a robust CNN based denoiser, namely Recursive Information Distillation Network (RIDNet), to handle the denoising task at high noise levels. The proposed RIDNet simultaneously keeps the efficiency and flexibility by introducing the information distillation module and merging a tunable noise level map as the input, respectively. Experiment results on Additive White Gaussian Noise (AWGN) images demonstrate that our method outperforms most of the state-of-the-art color image denoisers.

1. Introduction

As one of the low level computer vision tasks, image denoising plays a major role in many regards, such as image pre-processing for high level computer vision tasks [2], testing platform for assessing image prior models and optimization methods [21, 35, 8], and so on. Similar as previous image denoising approaches [20, 4, 19, 6, 29, 30], in this paper we adopt AWGN with a given noise level. There are two reasons: first, AWGN is a natural choice when there is no specific idea with noise source; second, real-world noise can be approximated as locally AWGN in a certain way [15]. Recently, Deep Learning (DL) based methods have been widely used for solving various inverse problems, such as image reconstruction, super-resolution and denoising [33, 34, 23, 28, 27], and great achievement in AWGN denoisers has been reached. These methods mainly focus on grayscale images and intend to learn the potential image prior as well as to fast inference from a training set of noisy images with corresponding ground-truth images [30]. However, when the input is color images (RGBs) that involve more semantic information and reliable representation for real scenes, simply employing the existing methods often fails to gain uniformly competitive denoising performance among effectiveness, efficiency and flexibility.

Many methods have been proposed to achieve high performance on one or two items among effectiveness, efficiency and flexibility of color image denoiser. These methods can be generally grouped into two categories, non-learning based methods and learning based ones. Representative methods of the former category include CBM3D [4], MCWNNM [26], and so on. CBM3D first classifies an image into groups of patches, then applies collaborative filtering to each group, and obtains the denoised image from the filtered patches at the end. MCWNNM is vector representation based CBM3D-like method. It introduces a weight matrix under the WNNM framework [8] to balance the contributions of R, G, and B channels according to their noise levels. Although above non-learning based methods achieve excellent denoising performance for color images, they suffer from several drawbacks, for example, time-consuming. On the other hand, learning based methods are recently dominated by CNN based methods [29, 30, 11]. From the viewpoint of regression, they are designed to learn a mapping function $x = F(y; \theta_\sigma)$ between the noisy input y and the desired output x. The model parameters θ_σ are trained for noisy images corrupted by AWGN with a preset noise level σ. DnCNN [29] obtains very competitive denoising performance, while FFDNet [30] is proposed later to additionally improve both the effectiveness and the flexibility. The prosperity of CNN for image denoising gives the credit to its superior modeling capacity and enormous progress in network training and design. However, existing CNN based denoising methods hardly ever achieve satisfying performance when encountering severe noise.

*Corresponding author
†Equal contribution
‡The authors are with College of Electronics and Information Engineering, the Shenzhen Key Laboratory of Advanced Machine Learning and Applications, the Guangdong Key Laboratory of Intelligent Information Processing, Shenzhen University, and School of Intelligent Systems Engineering, Sun Yat-sen University.

They are limited by the lack of network capability that these networks always contain just several layers. Hence, we propose a deeper network to deal with the color images suffering from severe noise, in which both the information distillation module [10] and the recursive learning strategy [13] are introduced to enjoy the efficiency. Furthermore, following the FFDNet, a tunable noise level map is taken into account as a part of the input to keep the flexibility of the proposed method.

We experimentally evaluate the proposed method on images corrupted by AWGN. Then we compare the proposed method with state-of-the-art color image denoising methods, such as CBM3D [4], DnCNN [29] and FFDNet [30]. The proposed method evidently performs better than the benchmark methods. More specially, comparing with the benchmark methods, the higher noise level is, the better denoising performance the proposed method can have. Meanwhile, the computational efficiency is well kept within a competitive range.

The rest parts of this paper are arranged as follows: Section 2 reviews the related work which not only comes from image denoising but also super-resolution. Section 3 presents our proposed color image denoising network which mainly benefits from the recursive information distillation modules. Section 4 demonstrates the experimental results as well as the comparison with others. Finally, Section 5 concludes this paper.

2. Related work

In this section, we first briefly review several recently proposed learning based AWGN denoiser, and then introduce two practical techniques for CNN based denoising methods.

2.1. Learning based AWGN denoiser

CNN based denoising methods have obtained outstanding performance to remove synthetic Gaussian noise. In [1], a method applying Multi-Layer Perceptron (MLP) was proposed to denoising task. In [3], a Trainable Nonlinear Reaction Diffusion (TNRD) model was proposed to remove Gaussian noise in various noise levels. MLP and TNRD are competitive non-blind AWGN denoisers that keep pace with CBM3D [4]. DnCNN [29] was proposed as a CNN based blind AWGN denoiser for the first time. It highlights the superiority of residual learning and batch normalization. After that, an effective CNN based model called FFDNet [30] was proposed by taking account the noise level map as a part of the network input. Later, a method [25] based on FFDNet was proposed to comprehensively analyze diverse techniques of FFDNet, and it implies that the use of residual learning is helpful for FFDNet. Recently, the denoising performance was boosted up with the help of semantic segmentation for distinguishing the foreground and background [17, 16]. In addition, a pixel-shuffle downsampling module was proposed to transform realistic noise to AWGN-like one [32], which efficiently results in the application of AWGN denoisers to realistic noise.

2.2. Information distillation

First proposed in [10] for Single Image Super-Resolution (SISR), Information Distillation Module (IDM) is famous for its superiority to capture plentiful and competent information. As shown in Figure 1, the IDM mainly consists of three parts: a local short-path information captor, a local long-path information captor and a compressing layer. The local short-path information captor contains the first three convolutional layers while the local long-path one contains another following three convolutional layers. Following each of the 3×3 convolutional layers there is a Leaky Rectified Linear Unit (LReLU) as the activation function, which is omitted in Figure 1. Additionally, between these two captors there are information split, separating the features along the channel, and feature concatenation. Following the latter captor there is a point-wise adding operation. By the cooperation of above modules, plentiful and competent features could be gradually obtained. Experimentally proved by the authors, IDM highly benefits the enhancement of the outline areas of an image when training the network. That is to say, IDM is suitable for learning the high frequency information which includes the noise inside a noisy image. Therefore, with residual learning [9], IDM could be excellently applied to image denoising, theoretically. Especially when several IDMs are cascaded, a deep but compact network is formed to reach great denoising performance with high efficiency.

2.3. Recursive learning

To keep the model parameters under control when increasing the depth of a network, recursive learning is adopted in SISR [13, 24]. Recursive learning is developed on the idea of parameter sharing, which is achieved by recursively calling the same module during the implementation of network training. To do so, the depth of a network increases by several times while the amount of parameters keeps unchanged. Hence, recursive learning is an effective technique to improve abundant feature retaining in a deep model without introducing additional parameters.

3. Proposed method

In this section, we first introduce the architecture of the proposed deep but compact network which mainly consists of several modified IDMs for color image AWGN denoising. Then the modified IDM and the loss function are introduced.

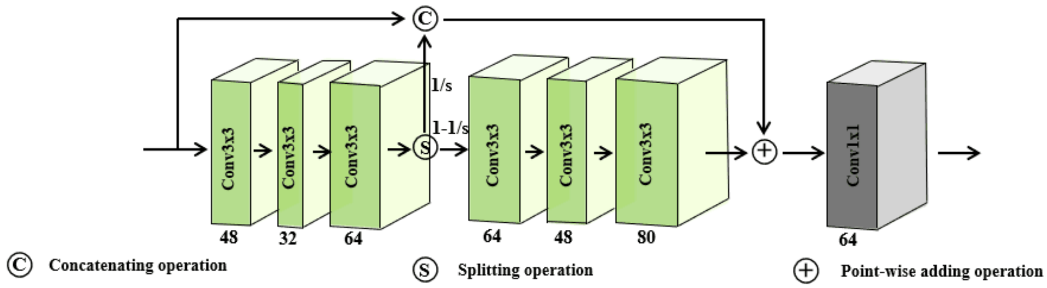

Figure 1. Structure of Information Distillation Module, feature maps are all in the same h×w size.

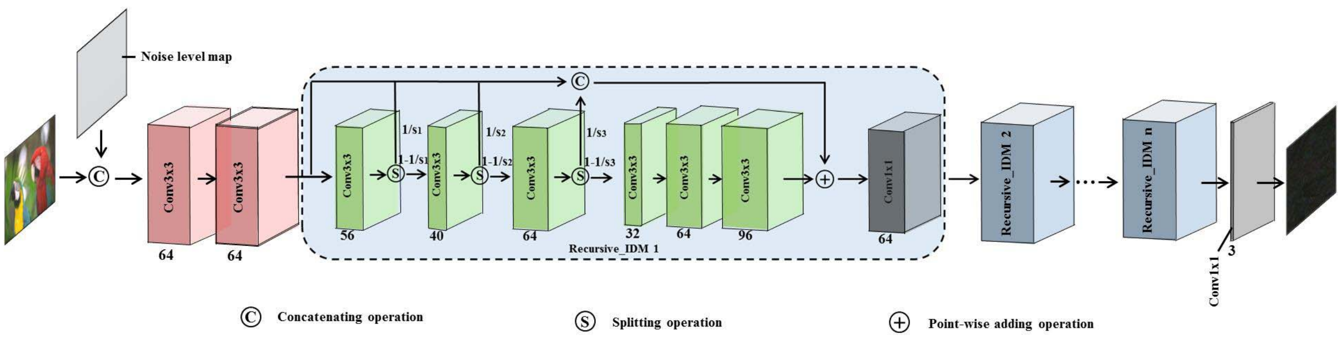

Figure 2. Structure of proposed network, feature maps are all in the same h×w size, and the network output is 3-channels estimating noise.

3.1. Network architecture

As shown in Figure 2 with different colors, our proposed network consists of three parts: two convolutional layers for feature extraction, N stacked modified IDMs and a 1×1 convolutional layer for feature compression. (1) Conv3×3: for the first two layers, 64 filters with size 3×3 are utilized to generate 64 feature maps. (2) Conv3×3 + LReLU: for layers except the last one inside each of the modified IDMs, different number of filters with size 3×3 are used, together with LReLU utilized for nonlinearity, which is omitted in Figure 2. (3) Conv1×1: for the last layer of each modified IDM and that of the whole network, 64 filters with size 1×1 and 3 filters with size 1×1 are used to compress the feature, respectively. In order to learn the noise to be removed, the whole network is in a residual learning form. Besides, as implied by FFDNet [30], jointly taking the noisy image and noise level as input makes sense for CNN to balance the noise remove and the detail maintenance. By doing so, it will largely boost up the flexibility of a single network. Hence, as shown in Figure 2, the input of our network is a noisy observation which is jointed with a noise level map when being fed into the network. However, the training model may suffer from visual artifacts caused by taking into a much higher noise level map as input, and we adopt the orthogonal initialization of the convolution filters [12] to suppress this difficulty.

3.2. Recursive information distillation modules

IDM in [10] shows the superiority to capture plentiful and competent information for SISR, and we take it into account to construct a deep network for color image denosing task by repeatedly stacking several IDMs. In order to better fit the target in color image denoising task, a modified IDM is proposed, as shown in the blue dashed box in Figure 2, to make good use of the multi-scale information. Comparing with the initial IDM shown in Figure 1, the modified IDM increases the filters of the first two layers from 48 and 32 to 56 and 40, respectively. Therefore, there comes out a deeper feature map, and part of it will be handed out for feature concatenation later. As for the local long-path information captor, the filters of the three layers are modified in a gradually increasing form, which specifically are 32, 64 and 96, respectively. Furthermore, in order to control the parameters of the network, recursive learning is adopted to share the parameters of each modified IDM. Hence, they are finally defined as the recursive information distillation modules in the proposed network named as Recursive Information Distillation Network (RIDNet).

3.3. Loss function

Experimentally proved by [16], different loss functions for one single denoising network may lead to different experimental results. Take the FFDNet as example, the L_1 loss function leads to the smoother flat areas, hence less low-frequency noise can be perceived. And the L_2 loss function better maintains detail information but perceives spotted artifacts in flat areas. As a residual network is constructed to learn the high-frequency information, the L_2 error is finally adopted to be the loss function of RIDNet, which is formulated as follows:

$$L(\boldsymbol{\theta}) = \frac{1}{2N} \sum_{i=1}^{N} ||R(\boldsymbol{y}_i; \boldsymbol{M}_i; \boldsymbol{\theta}) - (\boldsymbol{y}_i - \boldsymbol{x}_i)||^2, \quad (1)$$

where $\boldsymbol{\theta}$ is the trainable parameters in the network, $[(\boldsymbol{y}_i, \boldsymbol{x}_i)]_{i=1}^{N}$ are N noisy-clean patch pairs of training images, and $\boldsymbol{M}_i$ is the i-th noise level map, in which $\boldsymbol{y}_i$ is extracted by adding AWGN to the original image $\boldsymbol{x}_i$.

4. Experiments

4.1. Training datasets

Following the FFDNet, we adopt the dataset including 400 images from the BSD dataset [22], 400 images from the validation set of ImageNet [5], and the 4,744 images from the Waterloo Exploration dataset [18] for training. Each image of the training dataset is applied to form the input-output pairs $[(\boldsymbol{y}_i, \boldsymbol{M}_i; \boldsymbol{x}_i)]_{i=1}^{N}$.

4.2. Testing datasets

The proposed method is evaluated on three widely-used datasets: BSD68 [22], Kodak24 [7], McMaster [31]. The BSD68 dataset contains 68 images with size 481×321 from the testing set of the BSD300 dataset. The Kodak24 dataset contains 24 images with size 768×512. The McMaster dataset is a widely-used dataset for color demosaicing, which consists of 18 cropped images with size 500×500. Compared to the Kodak24 images, the images in McMaster dataset introduce more abundant colors [31], and is more challenging for color image denoising task.

4.3. Implementation details

Taking into account the performance and training efficiency, the total number of epochs is set to 80, and in each epoch, $64 \times 8,000$ patches are randomly cropped from the training images. The patch size should be larger than the receptive field of the network, which is set to 40×40 for avoiding over-fitting as well. The noisy patches are extracted by corrupting the clean patches with the uniform AWGN of noise level $\sigma \in (0, 75)$. Since the RIDNet is a fully convolutional one, it succeeds to the local connectedness that the output pixel depends on the local noisy input and local noise level. Hence, the trained network is talented to handle spatially variant noise by giving a non-uniform noise level map.

The ADAM algorithm [14] with default parameters setting is adopted to optimize network by minimizing the above loss function. The learning rate starts from 10^{-3} and reduces to 1/10 of itself every time the epoch number reaches the milestones (30, 50, 60), so the final learning rate comes to be 10^{-6}. The mini-batch size is set to 64, and the models are trained in Pytorch environment with an Nvidia TitanX GPU. The training of a single model can be done within one day.

4.4. Experimental results and comparison

In this subsection, we evaluate the RIDNet on noisy color images corrupted by AWGN. And we mainly compare our proposed method with state-of-the-art methods CBM3D [4], DnCNN [29] and FFDNet [30] and the improved FFDNet (Im-FFDNet) [25]. Tables 1, 2 and 3 report the testing results on CBSD68, Kodak24, and McMaster datasets with different noise levels, respectively. Note that the results of CBM3D, CDnCNN, and FFDNet are directly obtained from [30], while the model of the Im-FFDNet is retrained on the same dataset adopted in this paper to fairly regain the testing results in above three tables. Besides, the qualitative comparison between Im-FFDNet and RIDNet is shown in Figure 3.

From the experimental results, one can observe as follows: first, RIDNet surpasses CBM3D by a large margin among all three datasets, which demonstrates the superiority of learning based methods over non-learning ones. Second, in terms of PSNR, RIDNet slightly outperforms the three learning based methods on CBSD68 dataset except when the noise level is extremely low, i.e., $\sigma \leq 15$. While on the other two datasets, RIDNet generally achieves a obvious gain ($> 0.1dB$) even the noise level is up to 75, which demonstrates the superiority of a deeper network to handle severe noise. Third, for the testing time, RIDNet costs only 0.1s to 0.3s to inference one single image on GPU, which means negligible time-consuming. Although the time-consuming is about two times longer compared with the Im-FFDNet, RIDNet owns a five times deeper network over its. Last but not least, as intuitively shown in Figure 3, RIDNet shows its superiority among edge information preserving, details retaining and visual artifacts avoiding. From the first row in Figure 3, RIDNet keeps the edge of the lip smoother, cause it owns a deeper network to capture more abundant feature. And from the second and third rows, RIDNet better maintains the details in the windows and the finger, caused by the local short-path and long-path captor inside modified IDM to capture vast contextual information. Finally from the last row, we can see that RIDNet introduces no visual artifacts.

On the basis of above observations, RIDNet serves as a more robust AWGN denoiser for color images. Especially when existing attack from serious noise, RIDNet can still overcome it effectively as well as keep the efficiency and flexibility.

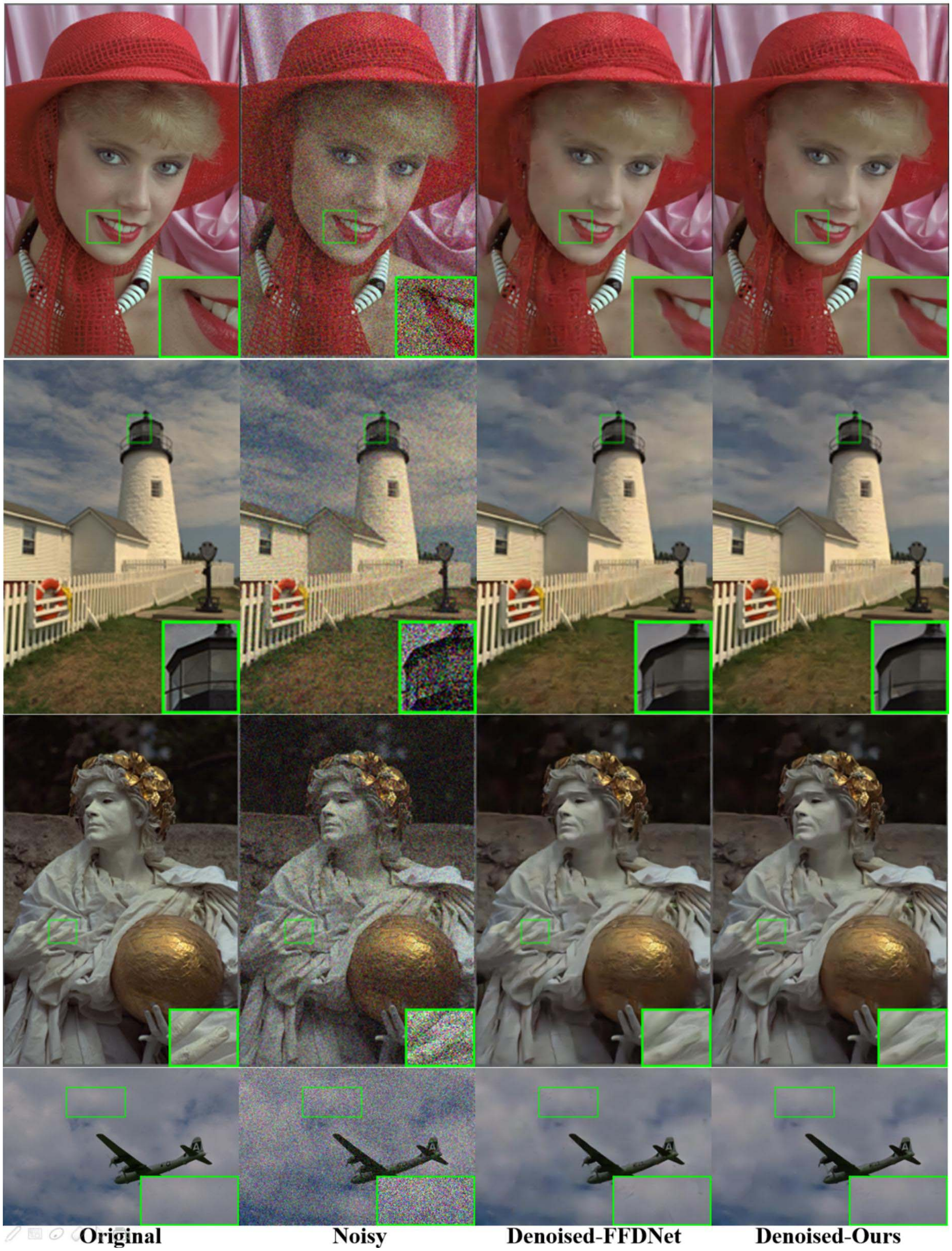

Figure 3. Color image denoising results ($\sigma = 50$) for comparison between Im-FFDNet and our RIDNet.

σ	Model	PSNR(dB)	SSIM	Testing time(s)
15	CBM3D	33.52	-	-
	DnCNN	33.89	-	-
	FFDNet	33.87	-	-
	Im-FFDNet	33.76	0.9643	0.07
	Ours	**33.83**	**0.9648**	**0.13**
25	CBM3D	30.71	-	-
	DnCNN	31.23	-	-
	FFDNet	31.21	-	-
	Im-FFDNet	31.17	0.9397	0.05
	Ours	**31.24**	**0.9406**	**0.13**
35	CBM3D	28.89	-	-
	DnCNN	29.58	-	-
	FFDNet	29.58	-	-
	Im-FFDNet	29.57	0.9171	0.06
	Ours	**29.64**	**0.9185**	**0.13**
50	CBM3D	27.38	-	-
	DnCNN	27.92	-	-
	FFDNet	27.96	-	-
	Im-FFDNet	27.97	0.8869	0.07
	Ours	**28.05**	**0.8893**	**0.13**
75	CBM3D	25.74	-	-
	DnCNN	24.47	-	-
	FFDNet	26.24	-	-
	Im-FFDNet	26.25	0.8439	0.07
	Ours	**26.36**	**0.8485**	**0.13**

Table 1. Experimental results on BSD68 dataset.

σ	Model	PSNR(dB)	SSIM	Testing time(s)
15	CBM3D	34.28	-	-
	DnCNN	34.48	-	-
	FFDNet	34.63	-	-
	Im-FFDNet	34.62	0.9646	0.12
	Ours	**34.75**	**0.9654**	**0.23**
25	CBM3D	31.68	-	-
	DnCNN	32.03	-	-
	FFDNet	32.13	-	-
	Im-FFDNet	32.21	0.9436	0.12
	Ours	**32.33**	**0.9449**	**0.23**
35	CBM3D	29.90	-	-
	DnCNN	30.46	-	-
	FFDNet	30.57	-	-
	Im-FFDNet	30.67	0.9241	0.12
	Ours	**30.80**	**0.9260**	**0.26**
50	CBM3D	28.46	-	-
	DnCNN	28.85	-	-
	FFDNet	28.98	-	-
	Im-FFDNet	29.12	0.8975	0.10
	Ours	**29.26**	**0.9007**	**0.25**
75	CBM3D	26.82	-	-
	DnCNN	25.04	-	-
	FFDNet	27.27	-	-
	Im-FFDNet	27.38	0.8583	0.11
	Ours	**27.57**	**0.8639**	**0.25**

Table 2. Experimental results on Kodak24 dataset.

σ	Model	PSNR(dB)	SSIM	Testing time(s)
15	CBM3D	34.06	-	-
	DnCNN	33.44	-	-
	FFDNet	34.66	-	-
	Im-FFDNet	34.53	0.9717	0.08
	Ours	**34.83**	**0.9731**	**0.17**
25	CBM3D	31.66	-	-
	DnCNN	31.51	-	-
	FFDNet	32.35	-	-
	Im-FFDNet	32.33	0.9564	0.06
	Ours	**32.57**	**0.9582**	**0.17**
35	CBM3D	29.92	-	-
	DnCNN	30.14	-	-
	FFDNet	30.81	-	-
	Im-FFDNet	30.84	0.9423	0.06
	Ours	**31.05**	**0.9446**	**0.16**
50	CBM3D	28.51	-	-
	DnCNN	28.61	-	-
	FFDNet	29.18	-	-
	Im-FFDNet	29.12	0.8975	0.06
	Ours	**29.06**	**0.9007**	**0.15**
75	CBM3D	26.79	-	-
	DnCNN	25.10	-	-
	FFDNet	27.33	-	-
	Im-FFDNet	27.38	0.8583	0.06
	Ours	**27.57**	**0.8639**	**0.16**

Table 3. Experimental results on McMaster dataset.

Dataset	Modeled by	Noise map	Multi scale	PSNR (dB)	SSIM
BSD 68	i-IDM	w	w/o	27.49	0.8761
	m-IDM1	**w**	**w**	**27.64**	**0.8804**
	m-IDM2	w	w/o	27.62	0.8799
	m-IDM3	w/o	w	27.52	0.8774
Kodak 24	i-IDM	w	w/o	28.62	0.8869
	m-IDM1	**w**	**w**	**28.86**	**0.8928**
	m-IDM2	w	w/o	28.83	0.8924
	m-IDM3	w/o	w	28.66	0.8886
Mc-Master	i-IDM	w	w/o	28.72	0.9141
	m-IDM1	**w**	**w**	**28.99**	**0.9189**
	m-IDM2	w	w/o	28.96	0.9185
	m-IDM3	w/o	w	28.79	0.9153

Table 4. Experimental results ($\sigma = 55$) of RIDNet with different components, i-IDM for the initial IDM, m-IDMx (x=1, 2 or 3) for the modified IDM, w for with, w/o for without and Multi scale for multi-scale information.

4.5. Ablation analysis

In this subsection, we further evaluate the effectiveness of different components in RIDNet. First, we respectively model the network by the initial IDM and by the modified IDM. In the same training and testing condition, experimental results are shown as the first two rows on each of the testing datasets in Table 4. It can be seen that the modified IDM surpasses the initial one by a large margin, which means the modified IDM can form a more robust network to deal with severe noise problem. Then, we test the impact of multi-scale information and noise level map, as shown in the last two rows on each of the testing datasets in Table 4, the experimental results demonstrate that they play an integral role in the modified IDM.

5. Conclusion

In this paper, we propose a deep but compact CNN called RIDNet for robust color image denoising. By stacking the recursive information distillation modules with accounting the noise level as input, RIDNet can simultaneously keep the effectiveness, efficiency and flexibility. Experimental results demonstrate that the RIDNet enjoys the superiority to get over severe noise effectively.

6. Acknowledgement

This work was supported in part by the NSFC Project under Grants 61771321, 61872429, 61871273 and 61701313, in part by the Guangdong Key Research Platform of Universities under Grants 2018WCXTD015, in part by the Science and Technology Program of Shenzhen under Grants KQJSCX20170327151357330, JCYJ20170818091621856, and JSGG20170822153717702, in part by the Interdisciplinary Innovation Team of Shenzhen University, and in part by the China Postdoctoral Science Foundation under Grants 2017M622778.

References

[1] Harold C Burger, Christian J Schuler, and Stefan Harmeling. Image denoising: Can plain neural networks compete with bm3d? In *2012 IEEE conference on computer vision and pattern recognition*, pages 2392–2399. IEEE, 2012.

[2] Priyam Chatterjee and Peyman Milanfar. Is denoising dead? *IEEE Transactions on Image Processing*, 19(4):895–911, 2009.

[3] Yunjin Chen and Thomas Pock. Trainable nonlinear reaction diffusion: A flexible framework for fast and effective image restoration. *IEEE transactions on pattern analysis and machine intelligence*, 39(6):1256–1272, 2016.

[4] K Dabov, A Foi, V Katkovnik, and K Egiazarian. Image denoising by sparse 3-d transform-domain collaborative filtering. image processing, ieee transactions on 16 (8), pp. 2080-2095. 2007.

[5] Jia Deng, Wei Dong, Richard Socher, Li-Jia Li, Kai Li, and Li Fei-Fei. Imagenet: A large-scale hierarchical image database. In *2009 IEEE conference on computer vision and pattern recognition*, pages 248–255. Ieee, 2009.

[6] Weisheng Dong, Lei Zhang, Guangming Shi, and Xin Li. Nonlocally centralized sparse representation for image restoration. *IEEE transactions on Image Processing*, 22(4):1620–1630, 2012.

[7] Rich Franzen. Kodak lossless true color image suite. *source: http://r0k. us/graphics/kodak*, 4, 1999.

[8] Shuhang Gu, Lei Zhang, Wangmeng Zuo, and Xiangchu Feng. Weighted nuclear norm minimization with application to image denoising. In *Proceedings of the IEEE conference on computer vision and pattern recognition*, pages 2862–2869, 2014.

[9] Kaiming He, Xiangyu Zhang, Shaoqing Ren, and Jian Sun. Deep residual learning for image recognition. In *Proceedings of the IEEE conference on computer vision and pattern recognition*, pages 770–778, 2016.

[10] Zheng Hui, Xiumei Wang, and Xinbo Gao. Fast and accurate single image super-resolution via information distillation network. In *Proceedings of the IEEE conference on computer vision and pattern recognition*, pages 723–731, 2018.

[11] Viren Jain and Sebastian Seung. Natural image denoising with convolutional networks. In *Advances in neural information processing systems*, pages 769–776, 2009.

[12] Kui Jia, Dacheng Tao, Shenghua Gao, and Xiangmin Xu. Improving training of deep neural networks via singular value bounding. In *Proceedings of the IEEE Conference on Computer Vision and Pattern Recognition*, pages 4344–4352, 2017.

[13] Jiwon Kim, Jung Kwon Lee, and Kyoung Mu Lee. Deeply-recursive convolutional network for image super-resolution. In *Proceedings of the IEEE conference on computer vision and pattern recognition*, pages 1637–1645, 2016.

[14] Diederik P Kingma and Jimmy Ba. Adam: A method for stochastic optimization. *arXiv preprint arXiv:1412.6980*, 2014.

[15] Jong-Sen Lee. Refined filtering of image noise using local statistics. *Computer graphics and image processing*, 15(4):380–389, 1981.

[16] Ding Liu, Bihan Wen, Jianbo Jiao, Xianming Liu, Zhangyang Wang, and Thomas S Huang. Connecting image denoising and high-level vision tasks via deep learning. *arXiv preprint arXiv:1809.01826*, 2018.

[17] Ding Liu, Bihan Wen, Xianming Liu, Zhangyang Wang, and Thomas S Huang. When image denoising meets high-level vision tasks: A deep learning approach. *arXiv preprint arXiv:1706.04284*, 2017.

[18] Kede Ma, Zhengfang Duanmu, Qingbo Wu, Zhou Wang, Hongwei Yong, Hongliang Li, and Lei Zhang. Waterloo exploration database: New challenges for image quality assessment models. *IEEE Transactions on Image Processing*, 26(2):1004–1016, 2016.

[19] Julien Mairal, Francis R Bach, Jean Ponce, Guillermo Sapiro, and Andrew Zisserman. Non-local sparse models for image restoration. In *ICCV*, volume 29, pages 54–62. Citeseer, 2009.

[20] Javier Portilla, Vasily Strela, Martin J Wainwright, and Eero P Simoncelli. Image denoising using scale mixtures of gaussians in the wavelet domain. *IEEE Trans Image Processing*, 12(11), 2003.

[21] Stefan Roth and Michael J Black. Fields of experts: A framework for learning image priors. In *2005 IEEE Computer Society Conference on Computer Vision and Pattern Recognition (CVPR'05)*, volume 2, pages 860–867. Citeseer, 2005.

[22] Stefan Roth and Michael J Black. Fields of experts. *International Journal of Computer Vision*, 82(2):205–229, 2009.

[23] Jo Schlemper, Guang Yang, Pedro Ferreira, Andrew Scott, Laura-Ann McGill, Zohya Khalique, Margarita Gorodezky, Malte Roehl, Jennifer Keegan, Dudley Pennell, et al. Stochastic deep compressive sensing for the reconstruction of diffusion tensor cardiac mri. In *International Conference on Medical Image Computing and Computer-Assisted Intervention*, pages 295–303. Springer, 2018.

[24] Ying Tai, Jian Yang, and Xiaoming Liu. Image super-resolution via deep recursive residual network. In *Proceedings of the IEEE conference on computer vision and pattern recognition*, pages 3147–3155, 2017.

[25] Matias Tassano, Julie Delon, and Thomas Veit. An analysis and implementation of the ffdnet image denoising method. *Image Processing On Line*, 9:1–25, 2019.

[26] Jun Xu, Lei Zhang, David Zhang, and Xiangchu Feng. Multi-channel weighted nuclear norm minimization for real color image denoising. In *Proceedings of the IEEE International Conference on Computer Vision*, pages 1096–1104, 2017.

[27] Guang Yang, Simiao Yu, Hao Dong, Greg Slabaugh, Pier Luigi Dragotti, Xujiong Ye, Fangde Liu, Simon Arridge, Jennifer Keegan, Yike Guo, et al. Dagan: deep de-aliasing generative adversarial networks for fast compressed sensing mri reconstruction. *IEEE transactions on medical imaging*, 37(6):1310–1321, 2017.

[28] S Yu, H Dong, G Yang, G Slabaugh, PL Dragotti, X Ye, F Liu, S Arridge, J Keegan, D Firmin, et al. Deep de-aliasing for fast compressive sensing mri (2017). *arXiv preprint arXiv:1705.07137*.

[29] Kai Zhang, Wangmeng Zuo, Yunjin Chen, Deyu Meng, and Lei Zhang. Beyond a gaussian denoiser: Residual learning of deep cnn for image denoising. *IEEE Transactions on Image Processing*, 26(7):3142–3155, 2017.

[30] Kai Zhang, Wangmeng Zuo, and Lei Zhang. Ffdnet: Toward a fast and flexible solution for cnn-based image denoising. *IEEE Transactions on Image Processing*, 27(9):4608–4622, 2018.

[31] Lei Zhang, Xiaolin Wu, Antoni Buades, and Xin Li. Color demosaicking by local directional interpolation and nonlocal adaptive thresholding. *Journal of Electronic imaging*, 20(2):023016, 2011.

[32] Yuqian Zhou, Jianbo Jiao, Haibin Huang, Yang Wang, Jue Wang, Honghui Shi, and Thomas Huang. When awgn-based denoiser meets real noises. *arXiv preprint arXiv:1904.03485*, 2019.

[33] Jin Zhu, Guang Yang, and Pietro Lio. How can we make gan perform better in single medical image super-resolution? a lesion focused multi-scale approach. *arXiv preprint arXiv:1901.03419*, 2019.

[34] Jin Zhu, Guang Yang, and Pietro Lio. Lesion focused super-resolution. In *Medical Imaging 2019: Image Processing*, volume 10949, page 109491L. International Society for Optics and Photonics, 2019.

[35] Daniel Zoran and Yair Weiss. From learning models of natural image patches to whole image restoration. In *2011 International Conference on Computer Vision*, pages 479–486. IEEE, 2011.